Controlled Under Pressure

DOI: 10.1002/anie.201202367

# Pressure-Driven Orbital Reorientations and Coordination-Sphere Reconstructions in $[CuF_2(H_2O)_2(pyz)]$**

*Alessandro Prescimone, Chelsey Morien, David Allan, John A. Schlueter, Stan W. Tozer, Jamie L. Manson, Simon Parsons,* Euan K. Brechin,* and Stephen Hill**

The application of pressure in the study of molecule-based materials has gained considerable recent interest, in part due to the high compressibilities of these materials, but also because the relevant electronic/magnetic (low-energy) degrees of freedom in such materials are often very sensitive to pressure.[1–11] For example, small changes in the coordination environment around a magnetic transition-metal ion can produce quite dramatic variations in both the on-site spin–orbit coupling as well as the exchange interactions between such ions when assembled into three-dimensional (3D) networks.[2–5] However, perhaps the most compelling reason to use pressure as a tool for understanding magneto-structural correlations is the possibility of focusing investigations on a single molecule or material, as opposed to using chemical means to influence the coordination environment around a metal center, for example, by studying families of seemingly related complexes that vary only in the identity of the coordinating ligands. The latter approach obviously suffers from the "non-innocence" of ligands, particularly in the solid state.

[*] Dr. A. Prescimone, Prof. S. Parsons, Prof. E. K. Brechin
EaStCHEM School of Chemistry, The University of Edinburgh
West Mains Road, Edinburgh, EH9 3JJ (UK)
E-mail: s.parsons@ed.ac.uk
ebrechin@staffmail.ed.ac.uk

C. Morien, Dr. S. W. Tozer, Prof. S. Hill
National High Magnetic Field Laboratory (NHMFL)
and Department of Physics
Florida State University, Tallahassee, FL 32310 (USA)
E-mail: shill@magnet.fsu.edu

Dr. D. Allan
Diamond Light Source, Harwell, Science Innovation Campus, Chilton (UK)

Dr. J. A. Schlueter
Materials Science Division, Argonne National Laboratory (USA)

Dr. J. L. Manson
Department of Chemistry and Biochemistry, Eastern Washington University (USA)

[**] We acknowledge support of the EPSRC (UK) and NSF (CHE-0924374). We thank Diamond Light Source for access to beamline I19 (proposal number MT6146). Work at Argonne, a U.S. Department of Energy Office of Science laboratory, is operated under Contract No. DE-AC02-06CH11357. Work performed at the NHMFL is supported by the NSF (DMR-0654118) and the State of Florida. J.L.M. gratefully acknowledges support of the NSF through Grant No. DMR-1005825. S.W.T. acknowledges support from DOE NNSA through DE-FG52-10A29659.

Supporting information for this article is available on the WWW under http://dx.doi.org/10.1002/anie.201202367.

The desire to study increasingly complex materials under pressure has spurred the development of sophisticated spectroscopic tools that can be integrated with high-pressure instrumentation.[12–15] The study of magneto-structural correlations requires not only precise crystallographic data, but also detailed spectroscopic information concerning the unpaired electron(s) that give(s) rise to the magnetic properties. Herein, we separately employ X-ray crystallography and high-frequency EPR spectroscopy to obtain high-resolution structural and magnetic data from oriented single-crystal samples subjected to pressures of up to 3.5 GPa.

We focus on the magnetic coordination polymer $[CuF_2(H_2O)_2(pyz)]$ (**1**, pyz = pyrazine), which previous powder diffraction studies have shown to undergo successive pressure-induced structural transitions, both of which are believed to involve dramatic reorientations of the Jahn–Teller (JT) axes associated with the $Cu^{II}$ ions.[9] Importantly, magnetic susceptibility studies reveal a pronounced change in the effective dimensionality of the extended Cu···Cu exchange interactions (from 2D to 1D) at the first of these transitions.[9] In the present investigation, EPR measurements provide direct information on the disposition of the magnetic $d_{x^2-y^2}$ orbital upon entering the first of the two high-pressure phases. Furthermore, while the previous powder X-ray studies established the onset of the phase transitions and the reorientations of the JT axes, we describe the results of single-crystal diffraction experiments, which not only yield structural data of substantially higher precision, but which also reveal the way in which relief of strain built-up in compressed H-bonds drives the system through successive phase transitions as pressure is increased. We also identify for the first time an additional high-pressure phase characterized by a dimerization of 1D chains.

Under ambient conditions complex **1** crystallizes in the monoclinic space group $P2_1/c$, with one copper center in the asymmetric unit (see Table S1 in the Supporting Information). The metal ion resides in a distorted octahedral environment formed by two O atoms from the two water molecules, two pyrazine N atoms, and two fluoride ions (Figure 1). The elongated JT axis lies along the N–Cu–N vector with the two symmetry-equivalent bonds measuring 2.454(6) Å; the shorter Cu–O and Cu–F distances are 1.984(4) Å and 1.908(4) Å, respectively (Table 1). The $Cu^{II}$ ions are linked into 1D chains along the crystallographic *a* axis through the pyrazine ligands. They are also linked into a 2D network within the *bc* plane by a series of short Cu–OH···F–Cu H-bonds [2.623(4) Å and 2.607(4) Å (Figure 1)]. The magnetic $d_{x^2-y^2}$ orbital associated with the axially elongated $Cu^{II}$ ion is expected to lie within the $CuF_2O_2$ (*bc*)

  

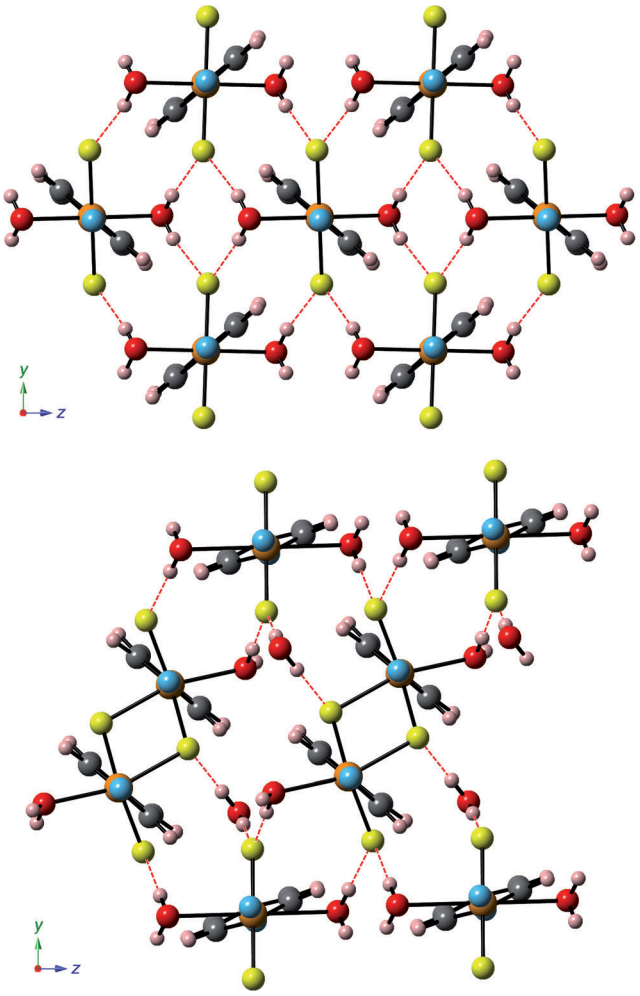


***Figure 1.*** Visualization of the 2D H-bonded network of **1** with the [O–H···F]$_2$ units in the crystallographic *bc* plane in phase I (top) and in phase IV (bottom). Color scheme: Cu = orange, O = red, F = yellow, N = blue, C = gray, H = salmon. The dashed red lines indicate the OH···F H-bonds.

***Table 1:*** Bond lengths [Å] in **1** as a function of pressure.

| *p* [GPa] | Cu1–F | Cu1–O | Cu1–N |
|---|---|---|---|
| 0 | 1.908(4) | 1.984(4) | 2.454(6) |
| 0.5 | 1.904(3) | 1.975(4) | 2.430(4) |
| 0.9 | 1.907(2) | 1.968(3) | 2.417(3) |
| 1.2 | 2.030(14) | 1.987(6) | 2.441(7) |
| 1.8 | 1.898(2) | 2.316(3) | 2.039(3) |
| 2.2 | 1.904(2) | 2.331(3) | 2.036(3) |
| 2.5 | 1.906(2) | 2.324(3) | 2.031(2) |
| 2.85 | 1.907(2) | 2.320(3) | 2.027(2) |
| 3.3 | 1.886(15) | 2.36(2) | 2.046(13) |
| | Cu2–F′ | Cu2–F | Cu2–F″ |
| 3.3 | 2.283(12) | 1.91(2) | 1.91(2) |
| | Cu2–O | Cu2–N | Cu2–N′ |
| 3.3 | 2.22(2) | 2.069(13) | 2.016(13) |

plane, thereby adding significance to the hydrogen bonding interactions. Indeed, extensive experimental studies of **1** at ambient pressures reveal a low-temperature transition to an antiferromagnetic state ($T_N = 2.54$ K) with strong 2D character, indicating appreciable Cu···Cu exchange within the *bc* plane, with considerably weaker interactions along the chains.[16] Under external hydrostatic pressure the first, and perhaps most obvious, effect is the compression of the unit cell (Table S1). At 1.2 GPa the Cu–X (X = N, F, O) distances remain essentially unchanged, but a contraction in both H-bonds to 2.515(13) Å is observed; this value is amongst the shortest having been observed for M–OH$_2$···F–M H-bonds, pinpointing the build-up of strain in the compressed intermolecular contacts.

Upon further increasing the pressure to 1.8 GPa, the expected phase modification occurs: the monoclinic symmetry is retained, but the Cu–N bonds are rather dramatically compressed (by 0.4 Å) to 2.039(3) Å, while the Cu–O bonds elongate (by 0.3 Å) to 2.316(3) Å. This is a clear indication that the JT axis has reoriented from the N–Cu–N vector to the O–Cu–O vector. This structural reorganization relieves the tension in the OH···F H-bonds, which increase to 2.702(3) Å and 2.626(3) Å, respectively. According to previous high-pressure studies performed on powder samples this phase change is reversible.[9,10] However, the single-crystal sample becomes polycrystalline upon release of the pressure. Moreover in the present investigation, the first phase modification is not observed until substantially higher pressures are achieved (about 1.8 GPa as opposed to 1.0 GPa[9]—see also the EPR data below). These differences may be due to the different pressure-transmitting media used for the various experiments, and possibly also due to the different nature of the samples (fine powder versus the more rigid single crystals). We note also that the pressures were calibrated at very different temperatures using different manometers.

Use of single-crystal diffraction data enables location of the H-atom positions from Fourier difference maps.[17] The mean Cu-O-H angle in phase II decreases from 108.3(9)° at 1.8 GPa to only 99.7(9)° upon further increasing the pressure to 2.85 GPa (Table S3). A search of the Cambridge Database shows that this almost perpendicular orientation is quite unusual.[18] Nevertheless, it preserves the near linearity in the OH···F contacts as the structure is compressed.

Further pressure increments reveal a second structural transition between 2.85 and 3.3 GPa, and this transformation is even more disruptive than the first. The two-fold symmetry is lost and the structure becomes twinned in the triclinic space group $P\bar{1}$ (Table S1). The cause of the symmetry loss lies in the ejection of one water molecule per copper unit from two thirds of the chains, forcing them to dimerize through the F atoms in order to fill the vacant coordination sites (Figure 1 and 2). Interestingly, the remaining one third of the chains are unchanged, that is, they have bond lengths and angles equivalent to those seen prior to the second phase transition. Consequently, the structure now contains two different chain types within the asymmetric unit. The structure is also twinned through a pseudo two-fold rotation about the *b* axis. The expelled water molecules remain in the crystal lattice, located between the monomeric and dimeric chains, held in place by the OH···F hydrogen bonding network (Figure S1). The mean O···F distance mediated by H-bonds is now 2.67(2) Å, spanning the range from 2.52(2) to 2.74(2) Å, while the average Cu-O-H angle is now 117.5(5)°.

  

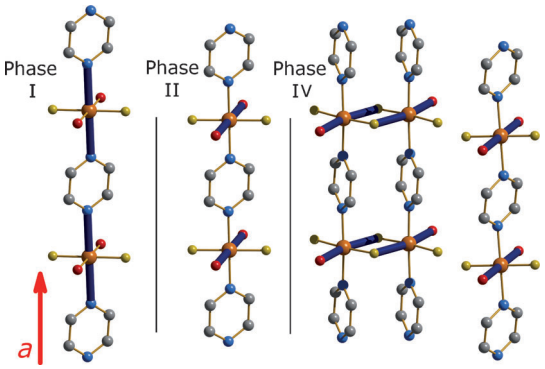


***Figure 2.*** Disposition of the JT axes (higlighted by the dark blue rods) in the three phases of **1**. Color scheme as for Figure 1.

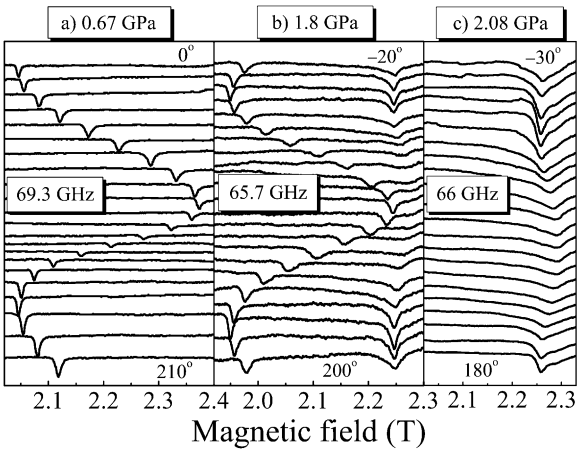


***Figure 3.*** Experimental EPR spectra recorded at 10 K as a function of the field orientation within the *ab* plane of a single crystal (transmission offset). The three panels correspond to three different pressures and microwave frequencies (indicated in the Figure). Spectra were recorded every 10°, with 0° corresponding to the field along *a*; the field orientations corresponding to the top and bottom traces are indicated in each panel.

The high-pressure phase obtained herein for a single crystal is different from phase III described by Halder et al.[9] The latter phase is monoclinic; the Cu atoms remain six-coordinate, but the JT axis shifts to the F–Cu–F direction. The powder pattern calculated from the triclinic structure described herein, which we shall call phase IV, is quite clearly different from the experimental powder data reported by Halder et al. (see Figure S2 in Reference [9]). It is possible that small deviations in hydrostaticity that arise from use of polycrystalline or single-crystal samples, or from the different hydrostatic media used in the two studies, are responsible for the differences in ours and Halder's results.

The transition to phase IV causes major changes in the coordination environment of the $Cu^{II}$ ions in the dimerized chains (Table 1): in particular, the JT axes are now oriented along the distorted O–Cu–F bonds (Figure 2), which also undergo a significant reorientation relative to the O–Cu–O JT axes associated with the monomeric chains. Most importantly, adjacent $Cu^{II}$ ions within the dimerized chains are now bridged directly by F atoms, which likely engenders appreciable exchange coupling between their unpaired electrons. The hydrogen bonding network is also affected: the Cu–OH···F–Cu pathways between the monomeric and dimerized chains remain relatively unaffected; however, the linkages between dimeric chains become considerably more complex (Figure S1).

The reorientation of the $Cu^{II}$ JT axes at the first pressure-induced transition has a profound influence on the magnetic properties of **1**. The consequent reorientation of the ground-state $d_{x^2-y^2}$ orbital into the $CuF_2N_2$ plane cuts off the 2D magnetic interactions within the *bc* plane, while promoting appreciable 1D correlations along the Cu–pyz–Cu chains. Previous magnetic susceptibility measurements have provided indirect evidence for this JT reorientation on the basis of a change in the dimensionality of the extended magnetic (Cu···Cu) interactions.[9]

On the other hand, single-crystal EPR studies can provide direct information on the symmetries of the wave functions associated with the unpaired magnetic electrons through their spin–orbit mixing with excited ligand-field states. This mixing manifests itself in a characteristic anisotropy of the Landé *g* tensor. EPR measurements were performed initially at a low pressure of 0.67 GPa. Figure 3a displays experimental spectra recorded as a function of field orientation at a frequency of 69.3 GHz and a temperature of 10 K. The crystal was oriented with its *c* axis approximately perpendicular to the plane of rotation, that is, the field was rotated in the *ab* plane. A single, sharp peak is observed that displays strong angle dependence with Landé-value extrema of $g_{\parallel} = 2.42$ and $g_{\perp} = 2.08$ (see Figure 4); the larger value corresponds to the direction parallel to the JT (*a*) axis. These values compare extremely well with data obtained under ambient conditions using a commercial X-band (9 GHz) spectrometer.[16]

The next set of measurements was performed at 1.82 GPa, with the 65.7 GHz data displayed in Figure 3b. This time, two signals are observed: one displays virtually identical angle dependence to the low-pressure signal (see Figure 4); however, the second signal displays a comparatively weaker angle dependence, with low *g* values in the 2.05 to 2.10 range, suggesting that it corresponds to field rotation within the plane of the $d_{x^2-y^2}$ orbital ($\perp$ orientation). Similar measurements were performed at a frequency of 96 GHz (Figure 4). These data provide the first hint that some fraction of the sample has transitioned into the second phase in which the JT axis switches to the O–Cu–O bonds. Nevertheless, the transition appears to be incomplete, which might signify a slight nonuniformity of the pressure within the cell. Also evident is a broadening of the EPR signal, particularly in the regions of maximum variation with angle. This indicates strains in the sample, that is, a degradation of the sample brought about either by thermal cycling or nonhydrostatic pressures within the cell.

Upon further increasing the pressure to 2.1 GPa (Figure 3c), the strongly angle-dependent signal (red/black data in Figure 4) vanishes completely, and the remaining EPR intensity is observed in a single, broad low-*g* signal (blue/green data in Figure 4). This high-pressure EPR signal displays a weak angle dependence (Figure 4) that agrees

  

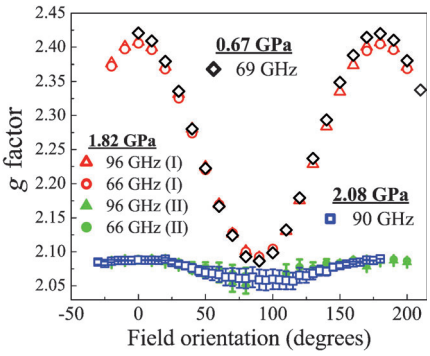


***Figure 4.*** EPR peak positions taken from Figure 3 (together with data obtained at other frequencies—not shown), plotted as their corresponding Landé *g* factors versus the orientation of the applied field within the *ab* plane of the crystal.

remarkably well with *bc*-plane rotations performed under ambient conditions.[16] However, in the present case, the field was rotated within the *ab* plane, thereby providing the most direct evidence that the magnetic $d_{x^2-y^2}$ orbital has switched from the $CuF_2O_2$ plane to the $CuF_2N_2$ plane. Unfortunately, efforts to access the second phase transition were hindered by multiple failures of the plastic pressure cells used for the EPR studies.[15] Future efforts that use diamonds with smaller culets will allow us to reach pressures in excess of 3 GPa more reliably.

We return to the second phase transition that occurs at about 3 GPa. As noted above, the dimerized chains involve direct Cu–F–Cu bridges, thus leading to the formation of $Cu_2F_2$ dimers that are coupled along the *a* axis through the pyrazine ligands. Magnetically, F-bridges have been shown to behave very much like OH-bridges;[19] the latter have been more widely characterized. In other words, the $Cu_2F_2$ dimers should have properties similar to those of their $Cu_2(OH)_2$ counterparts, for which extensive information can be found in the literature. On this basis, the Cu-F-Cu bridging angle of 104° would seem to suggest antiferromagnetic coupling; ferromagnetism is typically limited to a narrow angle range between 96° and 98°. Consequently, the dimerized chains can likely be viewed as antiferromagnetic spin ladders with different exchange-coupling strength on the rungs and along the rails, the latter determined by the pyrazine bridges. Such chains would very likely have a spin gap separating a singlet (diamagnetic) ground state from a band of dispersive triplet excited states;[20] the magnitude of this gap would be dependent on the ratio of the two exchange constants ($J_{rung}$:$J_{ladder}$), as well as their magnitudes. Consequently, the dimerized chains would most likely **not** contribute to the low-temperature magnetic susceptibility or the EPR response. Because the monomer chains are essentially indistinguishable from those in the intermediate-pressure phase, it is conceivable that the only magnetic signature of the second phase transformation would be a reduction of the susceptibility (or loss of EPR intensity) by a factor of three due to the dimerization of two thirds of the –Cu–pyz– chains.

It should be emphasized that the above discussion of the magnetism within the high-pressure phase is somewhat speculative. Efforts are currently under way aimed at measuring the pressure dependence of the magnetic susceptibility of a crystal in phase IV in order to bolster our understanding. We also hope that the present investigation may motivate ab initio calculations aimed at estimating the magnetic exchange interactions within the dimerized spin ladders, thereby providing a means of confirming whether the interaction within the $Cu_2F_2$ dimers is indeed antiferromagnetic. Such information could then be used to determine the magnitude of the spin gap associated with the dimerized chains. Finally, we note that high magnetic fields could eventually prove very useful for closing the singlet–triplet gap,[20] thereby "switching-on" the magnetism associated with the dimerized chains.

Received: March 26, 2012
Published online: May 29, 2012

**Keywords:** copper · EPR spectroscopy · high-pressure chemistry · Jahn–Teller reorientation · structure elucidation

[1] D. S. Clarke, S. P. Strong, P. M. Chaikin, E. I. Chashechkina, *Science* **1998**, *279*, 2071.
[2] W. Fujita, K. Awaga, *Mol. Cryst. Liq. Cryst. Sci. Technol. Sect. A* **2000**, *341*, 389.
[3] M. Mito, H. Deguchi, T. Tajiri, M. Yamashita, H. Miyasaka, *Phys. Rev. B* **2005**, *72*, 144421.
[4] A. Sieber, R. Bircher, O. Waldmann, G. Carver, G. Chaubousant, H. Muttka, H.-U. Güdel, *Angew. Chem.* **2005**, *117*, 4311; *Angew. Chem. Int. Ed.* **2005**, *44*, 4239.
[5] a) A. Prescimone, C. J. Milios, J. Sanchez-Benitez, K. V. Kamenev, C. Loose, J. Kortus, S. A. Moggach, M. Murrie, J. E. Warren, A. R. Lennie, S. Parsons, E. K. Brechin, *Dalton Trans.* **2009**, 4858.
[6] K. W. Galloway, S. A. Moggach, P. Parois, A. R. Lennie, J. E. Warren, E. K. Brechin, R. D. Peacock, R. Valiente, J. González, F. Rodriguez, S. Parsons, M. Murrie, *CrystEngComm* **2010**, *12*, 2516.
[7] S. A. Moggach, S. Parsons, *Spectrosc. Prop. Inorg. Organomet. Compd.* **2009**, *40*, 324.
[8] P. Parois, S. A. Moggach, J. Sanchez-Benitez, K. V. Kamenev, A. R. Lennie, J. E. Warren, E. K. Brechin, S. Parsons, M. Murrie, *Chem. Commun.* **2010**, *46*, 1881.
[9] G. J. Halder, K. W. Chapman, J. A. Schlueter, J. L. Manson, *Angew. Chem.* **2010**, *122*, 429; *Angew. Chem. Int. Ed.* **2010**, *49*, 419, and references therein.
[10] J. L. Musfeldt, Z. Liu, S. Li, J. Kang, C. Lee, P. Jena, J. L. Manson, J. A. Schlueter, G. L. Carr, M.-H. Whangbo, *Inorg. Chem.* **2011**, *50*, 6347.
[11] A. L. Leitch, K. Lekin, S. M. Winter, L. A. Downie, H. Tsuruda, J. S. Tse, M. Mito, S. Desgreniers, P. A. Dube, S. Zhang, Q. Liu, C. Jin, Y. Ohishi, R. T. Oakley, *J. Am. Chem. Soc.* **2011**, *133*, 6051.
[12] L. Merrill, W. A. Bassett, *Rev. Sci. Instrum.* **1974**, *45*, 290.
[13] A. Dawson, D. R. Allan, S. Parsons, M. Ruf, *J. Appl. Crystallogr.* **2004**, *37*, 410.
[14] J. Diederichs, A. K. Gangopadhyay, J. S. Schilling, *Phys. Rev. B* **1996**, *54*, R9662.
[15] D. E. Graf, R. L. Stillwell, K. M. Purcell, S. W. Tozer, *High Pressure Res.* **2011**, *31*, 533.
[16] J. L. Manson, M. M. Conner, J. A. Schlueter, A. C. McConnel, H. I. Southerland, I. Malfant, T. Lancaster, S. J. Blundell, M. L.

  

Brooks, F. L. Pratt, J. Singleton, R. D. McDonald, C. Lee, M.-H. Whangbo, *Chem. Mater.* **2008**, *20*, 7408.
[17] P. W. Betteridge, J. R. Carruthers, R. I. Cooper, K. Prout, D. J. Watkin, *J. Appl. Crystallogr.* **2003**, *36*, 1487.
[18] F. H. Allen, *Acta Crystallogr. Sect. B* **2002**, *58*, 380.
[19] S. C. Lee, R. H. Holm, *Inorg. Chem.* **1993**, *32*, 4745.
[20] T. Giamarchi, A. M. Tsvelik, *Phys. Rev. B* **1999**, *59*, 11398.

  